EurJOC
European Journal of Organic Chemistry

Research Article
doi.org/10.1002/ejoc.202400861

Chemistry Europe
European Chemical Societies Publishing

www.eurjoc.org

Structure-Based Design and in-Flow Synthesis of Aromatic Endoperoxides Acting as Oxygen Releasing Agents

Marco Agnes,*[a] Adelaide Santagata,[a] Daniele Veclani,[a] Alessandro Venturini,[a] Magda Monari,[b] Paolo Dambruoso,[a] and Ilse Manet*[a]

Hypoxia occurs in different pathological settings as a consequence of poor vascularization, and it results in reduced efficacy of some current nosocomial treatments i.e. chemotherapy and photodynamic therapy. In order to overcome these boundaries, aromatic endoperoxides (EPOs) have been studied and proposed as oxygen-releasing agents (ORAs) due to their ability to reversibly bind molecular oxygen (O_2), liberating it upon suitable triggering. DFT calculation of the dissociation energy (E_{diss}) of the intramolecular O–O bridge and structural crystallographic data of synthesized and studied EPOs drove the design of an array of 9,10-disubstituted anthracenes among which three candidates were carefully selected. Once optimized the synthesis of the aromatic substrates, for the first time the corresponding EPOs have been produced under continuous flow irradiation in the presence of a sub-stoichiometric amount of a photosensitizer in organic solvents. The release of O_2 could be obtained straightforwardly at 37.5 °C by thermolysis. In accordance with the calculated $E_{diss} = 3.2$ kcal mol^{-1} and an experimental $t_{1/2} = 40$ minutes, 3,3′-(anthracene-9,10-diyl)bis(prop-2-yn-1-ol) resulted as the best candidate for the sustained release of O_2 under physiologically relevant conditions. Its exploitation as ORA to relieve hypoxia will be evaluated and described in due course.

Introduction

Hypoxia is a condition occurring in several disorders resulting in lower levels (1–5%) of molecular oxygen (O_2) compared to the normoxic conditions of healthy physiological environment, where the O_2 tension is typically between 10 and 21%.[1] This status is mainly induced by the poor vascularization or impaired blood flow characterizing potentially fatal illnesses like solid tumors,[2,3] microbial[4] and fungal[5] infections and biofilms, cerebral[6] and myocardial[7] ischemia, *etc.* The harshness of hypoxia resides in its ability to annihilate the efficacy of current drug-based therapies as it boosts drug resistance[4] and to reduce the effects of radiotherapy[8] and photodynamic therapy (PDT)[9] as well.

In order to overcome hypoxia-related limitations, the design and development of biocompatible molecular vectors able to deliver O_2 directly to the target tissues is gaining significant attention in the pharmacological field.[9] In this context, an increasing amount of literature focused on aromatic endoperoxides (EPOs) as suitable Oxygen-Releasing Agents (ORAs).[10] The polycyclic aromatic precursors are cheap, versatile substrates able to reversibly bind and release O_2 when properly functionalized and stimulated. The chemistry of these interesting EPOs has been deepened in the past[11] and many aspects regarding their preparation and reactivity are now well-known and established.[12] Among others, the group of W. Fudickar and T. Linker was able to produce a remarkable amount of EPOs from both anthracene[13,14] and naphthalene[15,16] derivatives.

The addition to polycyclic aromatic precursors of singlet oxygen ($^1O_2$) photochemically generated *in situ* upon irradiation of the reaction mixture containing a sub-stoichiometric amount of a photosensitizer (PS), is the most efficient way to form EPOs.[10] This photooxygenation reaction is straightforward and typically results in final products bearing the target intramolecular O–O bridge. Selection and positioning of the substituents on the aromatic cores are crucial for the overall ability to selectively bind and release O_2.

The smooth release of O_2 either in its triplet or singlet state is usually induced by thermolysis, driving to the restoration of the parent aromatic precursors.[17] However, being these molecules studied in parallel for applications in the fields of electronic[18] and optical[19] devices, organic semiconductors[20] and printing,[21] the design of EPOs usually does not consider biocompatibility and often the temperatures needed for triggering the O_2 release are above 50 °C.

In a previous work,[22] a series of anthracene or naphthalene derivatives were synthesized and tested as ORAs (Figure 1). Compared to previously published literature,[23] effective improvements were achieved in the photooxygenation of mono- and di-substituted anthracene derivatives, namely 4-(anthracen-9-yl)benzoic acid, **ANBA**, and 4-(10-phenylanthracen-9-yl)benzoic acid, **PABA**, respectively, forming more stable EPOs

[a] M. Agnes, A. Santagata, D. Veclani, A. Venturini, P. Dambruoso, I. Manet
Istituto per la Sintesi Organica e la Fotoreattività (ISOF), Consiglio Nazionale delle Ricerche (CNR), Via Gobetti 101, 40129 Bologna, Italy
E-mail: marco.agnes@isof.cnr.it
ilse.manet@isof.cnr.it

[b] M. Monari
Dipartimento di Chimica "Giacomo Ciamician", Alma Mater Studiorum – Universita' di Bologna, Via P. Gobetti 85, 40129, Bologna, Italy

Supporting information for this article is available on the WWW under https://doi.org/10.1002/ejoc.202400861

Research Article
doi.org/10.1002/ejoc.202400861

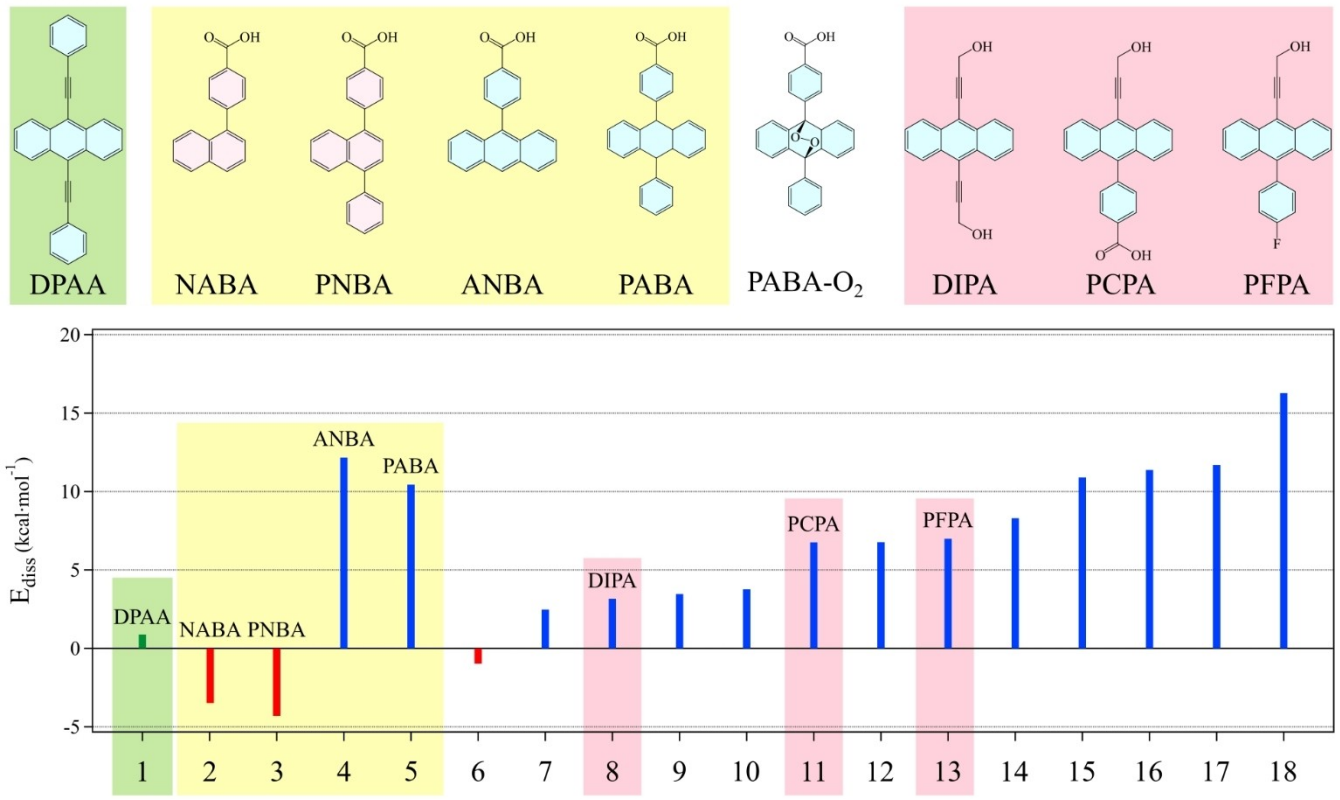

Figure 1. *Top panel*: chemical structure of reference compound (green background) 9,10-diphenylalkynylanthracene (**DPAA**); previously reported compounds (yellow background): 4-(naphthalen-1-yl)benzoic acid, **NABA**, 4-(4-phenylnaphthalen-1-yl)benzoic acid, **PNBA**, 4-(anthracen-9-yl)benzoic acid, **ANBA**, 4-(10-phenylanthracen-9-yl)benzoic acid, **PABA**, 9,10-endoperoxide of PABA, **PABA-O2**; newly synthesized compounds (pink background): 3,3′-(anthracene-9,10-diyl)bis(prop-2-yn-1-ol), **DIPA**, 4-(10-(3-hydroxyprop-1-yn-1-yl)anthracen-9-yl)benzoic acid, **PCPA**, 3-(10-(4-fluorophenyl)anthracen-9-yl)prop-2-yn-1-ol, **PFPA**. *Bottom panel*: Plot of the dissociation energies (E_{diss}, kcal mol^{-1}) for a series of anthracene derivatives obtained by density functional theory (DFT) B3LYP/Def-TZP/dichloromethane calculations (see Table S2 for correlating the numbers to the structures).

compared to the analogous naphthalene-derivatives, 4-(naphthalen-1-yl)benzoic acid, **NABA**, and 4-(4-phenylnaph-thalen-1-yl)benzoic acid, **PNBA**. Out of four, only **PABA-O2** was found to release O_2 effectively, when heated at 90 °C for a prolonged time.

Herein, computational and crystallographic data were used to select the most suitable structural features to improve the ORA performances in terms of EPO formation and O_2 release. For the first time, the synthesis of anthracene-based EPOs bearing carefully selected substituents was carried out using a continuous flow photochemical reactor allowing to envisage the industrial scale up of the photooxygenation step (Figure S1). Importantly, as anticipated by computational insights, these EPOs release O_2 in physiologically compatible conditions thus suggesting the possibility to further explore these molecules as ORAs for relieving hypoxia.

Results and Discussion

Computational Studies

The aim of the computational analysis was to screen an array of aromatic derivatives consisting of previously published compounds taken as reference[22,24] and new proposed structures which were envisaged to have better performances as ORA at physiologically relevant conditions.

It is established that the electronic character, position and size of substituents have a direct influence on the kinetics of formation, regiochemistry and stability of aromatic EPOs.[25] In particular, considering a concerted mechanism of the [4 + 2] reaction between the aromatic substrates and the $^1O_2$ generated *in situ*,[11] their readiness to bind and release O_2 can be directly related to the dissociation energy (E_{diss}) calculated using the density functional theory (DFT).[26–28] The computed E_{diss} of the EPOs of **NABA** and **PNBA** resulted to be −3.49 kcal mol^{-1} and −4.31 kcal mol^{-1}, respectively, while in the case of **PABA** and **ANBA** it was found to be 10.44 kcal mol^{-1} and 12.16 kcal mol^{-1}, respectively (Figure 1, Table S2). The negative values obtained for **NABA** and **PNBA** confirmed the lack of any stabilizing effect observed experimentally as the formation of the O–O bridge could not be detected. The opposite behaviour of **PABA** and **ANBA** with large positive E_{diss} values is in line with the straightforward formation of EPOs in solution and, above all, their high stability. In fact, only heating at 90 °C for several hours afforded the clean release of O_2 from **PABA-O2** with similar performances in organic solvent and water, upon complexation with a polymeric matrix.[22]

Despite the well-known effect of electron-withdrawing (EWGs) or electron donating groups (EDGs) on the rate of formation and stability of aromatic EPOs, **ANBA**, **PABA**, **NABA** and **PNBA** decorated with the same substituents oriented perpendicular to the conjugated cores thus reducing the electronic effect, showed quite divergent calculated E_{diss}. Hence DFT analysis was further meant to verify if steric interactions could contribute to the overall binding process thanks to the use of 2D and 3D color-filled reduced gradient density (RGD) projections (Figure S3). No major differences could be found between the two sets of molecules in the intensity of VdW and steric interactions. However, the aromatic substituents on **NABA** and **PNBA** are less tilted compared to the anthracene analogues, lowering the possibilities to establish any interaction and thus resulting in the impossibility to observe such EPOs experimentally.

In light of these results, the focus of the predictive analysis was narrowed to the anthracene-based EPOs, seeking for substrates displaying $E_{diss} < 10$ kcal mol^{-1}. 9,10-diphenylalkynylanthracene (**DPAA**) has been reported to have a half-life ($t_{1/2}$) of 23 minutes at 25 °C in toluene.[25] Being this value closer to our goal of sustained release of O_2 at 37.5 °C, its calculated $E_{diss} =$ 0.88 kcal mol^{-1} was taken as lower limit. Moreover, considering the application as therapeutic agents, fully hydrophobic molecules were not taken into consideration, while the presence of hydroxylic, carboxylic and more hydrophilic functional groups was preferred in order to boost their water solubility and/or allow further functionalization. A total of 13 anthracene structures bearing different combination of EDGs or EWGs were tested and compared with **DPAA**, **PABA** and **ANBA** (Table S2).

Among the newly designed molecules (entries 6–18 in Table S2), structure **6**, bearing a tris-trifluoromethyl-benzene at position 9 and a prop-2-yn-1-ol moiety at position 10 showed a negative E_{diss} value $= -0.98$ kcal mol^{-1} (Figure 1) induced by unfavourable steric effects (Figure S4) and it was not further considered. Structures **7** to **10**, bearing the prop-2-yn-1-ol group(s) in position 9 and/or 10, showed interesting E_{diss} ranging from 2.47 to 3.77 kcal mol^{-1}, expected to have a slightly higher stability compared to **DPAA**. Structures **11** to **14** exhibited remarkable E_{diss} between 6.75 and 8.30 kcal mol^{-1}, while structures **15** to **18** displayed $E_{diss} > 10.89$ kcal mol^{-1} thus they were not further considered.

Eventually, three molecules, **8**, **11** and **13**, were selected to be synthesized as suitable ORA candidates, namely:

8. 3,3′-(anthracene-9,10-diyl)bis(prop-2-yn-1-ol), **DIPA** ($E_{diss} =$ 3.16 kcal mol^{-1})

11. 4-(10-(3-hydroxyprop-1-yn-1-yl)anthracen-9-yl)benzoic acid, **PCPA** ($E_{diss} = 6.75$ kcal mol^{-1})

13. 3-(10-(4-fluorophenyl)anthracen-9-yl)prop-2-yn-1-ol, **PFPA** ($E_{diss} = 6.98$ kcal mol^{-1})

Symmetrical **DIPA**, bearing prop-2-yn-1-ol moieties in positions 9 and 10 is expected to release O_2 at low temperature and to be more suitable for further functionalization and increased water solubility thanks to the terminal hydroxyl groups. Unsymmetrical **PCPA** and **PFPA**, bearing a prop-2-yn-1-ol moiety in position 9 and a *para* benzoic acid or a *para* fluorophenyl group, respectively, in position 10, were supposed to generate EPOs more stable than **DIPA**, but more labile than **PABA**. The different ionisable and non ionisable appendages may be an interesting feature to regulate their solubility and further covalent or non-covalent manipulation.

X-Ray Crystallographic Analysis

Single crystal analysis identified structural, distinctive features for anthracene and naphthalene derivatives regarding the relative position of the aromatic cores and substituents (Figure 2).

ANBA and **PABA** crystallized with a single molecule per asymmetric unit and almost orthogonal dihedral angles between the anthracene plane and the aromatic substituents: 82.84(4)° for **ANBA**; 87.5 and 83.1(2)° for **PABA** (Figure 2a). **PFPA** crystallized with two molecules per asymmetric unit and the aromatic substituent is oriented at 77.2(1)° with respect to the anthracene plane. One O–H···O hydrogen bond links together the two conformers present in the asymmetric unit and a non-classical intermolecular H bond (C–H···F) was observed (Figure S5). **PABA-O2** showed loss of planarity in the central ring of the anthracene unit due to the formation of the O–O bond with the C atoms bound to the substituents that, instead, maintain their orientation (Figure 2c). Moreover, its crystalline and calculated structures overlap significantly, suggesting no major differences between the conformation of the EPO as a solid and in solution.

In the case of naphthalene derivatives, the crystal structure of **NABA** was found to match previously published data (Figure S2),[29] displaying a dihedral angle of 46.8°. Interestingly, **PNBA** crystallized adopting six different conformers (Figure 2d). The dihedral angles between the phenyl rings and the naphthalene skeleton range from 65.85 to 46.75(5)° whereas the dihedral angles between the benzoic acid rings and the naphthalene moiety range similarly from 45.88 to 59.49(5)°. In the solid state of **PNBA**, two distinct arrangements are present: one in which the two aromatic substituents are aligned (mutual dihedral angles from 17.83 to 20.23(5)°) and one in which they are oriented in different directions (mutual dihedral angles from 65.09 to 75.18(5)°) presumably to optimize packing effects.

In accordance with DFT calculations and experimental data, the relative orientation of the substituents should be more favorable for anthracene derivatives, empowering the choice of the target candidates.

Synthesis of Aromatic Substrates

The synthesis of symmetrical and unsymmetrical alkynyl-bearing anthracene derivatives was achieved by Sonogashira[24,25] and Suzuki[22] couplings adapting published procedures and using 9,10-dibromoanthracene (**DBA**) as starting material (Scheme 1).

Formation and isolation of the mono-substituted 9-bromo-10-prop-2-yn-1-ol-anthracene (**BPYA**) after Sonogashira reaction in the presence of propargyl alcohol was relatively straightfor-

Research Article
doi.org/10.1002/ejoc.202400861

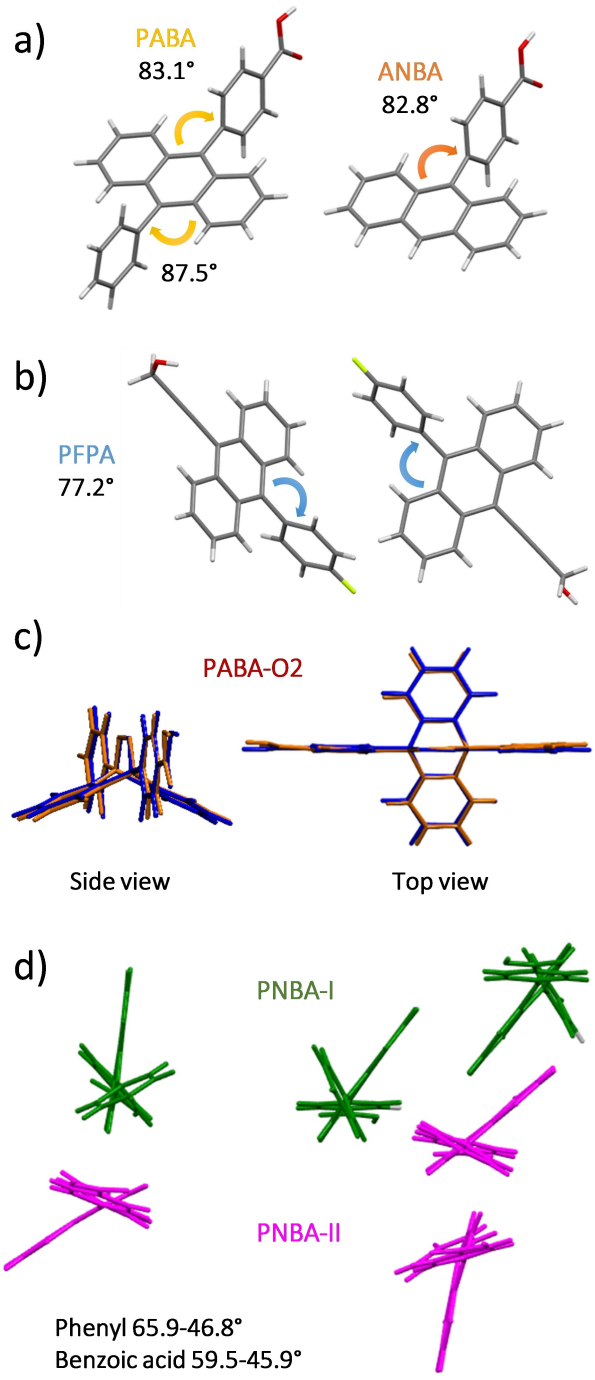

Figure 2. a) Crystal structures of **PABA** and **ANBA**. b) Asymmetric unit of **PFPA** crystals. c) Superimposed calculated (blue) and crystalline (orange) structures of **PABA-O2**. d) Asymmetric unit of **PNBA** crystals, composed of six different molecules, divided into two subgroups according to the different angle between substituents: PNBA-I (green structures): 65.1 – 75.2 °, PNBA-II (magenta structures): 17.8 – 20.2 °.

ward and the intermediate was obtained with a 27% yield. In order to obtain **DIPA**, the same reaction was left with enough equivalents of reactants for a prolonged time in order to substitute the remaining bromine atom eventually reaching the double substitution with an overall yield of 27%.

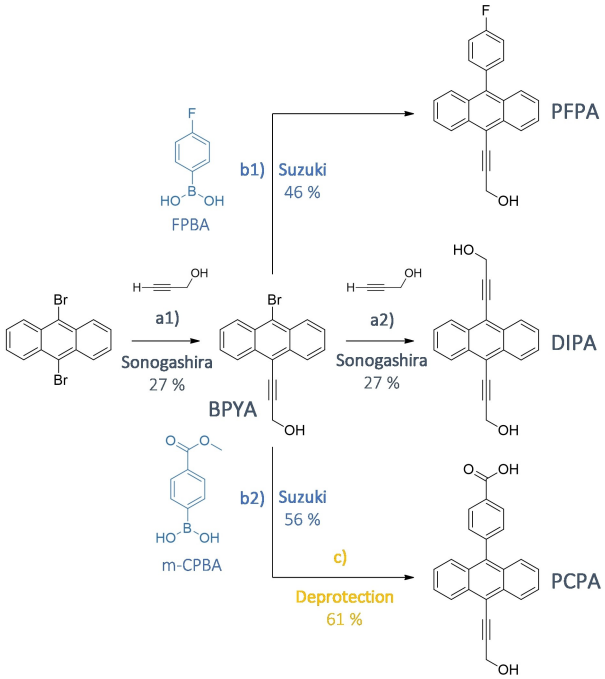

Scheme 1. Synthetic steps for the synthesis of **DIPA**, **PFPA** and **PCPA**. *Sonogashira coupling* (step a): $Pd(PPh_3)_2Cl_2$, CuI, diisopropylamine, propargyl alcohol, THF, reflux. *Suzuki coupling* (step b): $Pd(PPh_3)_4$, $CsCO_3$ 2 $M_{(aq.)}$, b1) (4-fluorophenyl)boronic acid (FPBA); b2) 4-(methoxycarbonyl)phenyl)boronic acid (m-CPBA), THF, reflux. Deprotection of methyl ester (step c): LiOH 2 $M_{(aq.)}$, MeOH, reflux.

Different approaches were tested in order to increase the yields of the final step:

- Two-step reaction, repeating the same procedure on isolated BPYA
- Protection of the -OH groups of the propargyl alcohol with tert-butyldimethylsilyl or trimethylsilyl groups
- Reduction of the amount of Cu2+ catalyst known to favor cross-coupling between alkynyl terminal moieties
- The use of organic bases others than di-isopropylamine, i.e. triethylamine.

None of the proposed changes led to significant improvements in the yield of the reaction (data not shown).

In order to synthesize **PFPA** and **PCPA**, the intermediate **BPYA** underwent Suzuki reactions with 4-fluorophenyl-boronic acid (FPBA) and 4-(methoxycarbonyl)phenyl)boronic acid (m-CPBA), respectively (Scheme 1). **PFPA** was isolated directly after column chromatography with a 46% yield, while the methyl-protected intermediate obtained in a 56% yield was treated with LiOH to eventually obtain the final product **PCPA** with a 61% yield. Detailed description of the synthetic procedures and full NMR and MS characterization of the products are shown in the SI.

Photooxygenation Step *in Flow*

The synthesis of aromatic EPOs has been optimized adapting a previously published procedure[22] to a photochemical reactor

Research Article
doi.org/10.1002/ejoc.202400861

equipped for continuous flow irradiation (Vapourtec® E-Series, see SI for detailed description of the instrument and the synthetic procedure). The interest of the synthetic organic community towards flow processes is rapidly growing for an increasing number of applied chemical processes.[30] In particular, photo-induced and catalyzed transformations capitalized on the use of this technology to improve reaction rate, yield and batch size, especially thanks to the massive surface-to-volume *ratio* enabling increased efficiency and homogeneity of irradiation.[31]

For our purpose, the reactor was endowed with a LED lamp emitting at 525 nm (±10 nm) and it enabled fine control of the light intensity, the inner reactor temperature and the flow rate, which could be adjusted according to the desired residence time.

First of all, the stability of the PS was tested in DCM:THF, 9:1 (Figure S6). The readily available methylene blue, MB, despite its low absorption at the selected wavelength ($\varepsilon_{525} \approx 4000\ M^{-1}cm^{-1}$) entirely bleached upon irradiation, while 5, 10, 15, 20-*tetrakis*(3-hydroxyphenyl)-porphyrin (mTHPP, $\varepsilon_{525} = 10000\ M^{-1}cm^{-1}$) was photostable under the same conditions. **PABA** was exploited as reference substrate for the photooxygenation step being its EPO analogue **PABA-O2** readily formed and easy to handle (Figure 3a). Various combinations of residence times, light intensities and molar *ratios* between **PABA** and PS (either MB or mTHPP) were tested in order to optimize the *in flow* reaction conditions with respect to the previously published procedure based on a 100 W Hg-lamp setup (Figures S7, S8). Eventually, the performance of the photochemical step *in flow* yielded quantitative formation of **PABA-O2** reducing 5 times the amount of PS (1% mol/mol) in only 10 minutes, resulting in a 6-fold faster reaction compared to previously reported batch conditions.[22] Moreover, the same performance was achieved by using 80% of the intensity of irradiating light enabling even milder reaction conditions.

All the tested anthracenes showed similar absorption profiles and their molar absorption coefficients (ε, $M^{-1}\,cm^{-1}$) were found in the range 15000±1500 for **PABA**, **PFPA** and **PCPA**, and about 28000 for **DIPA** (Figure 3b). Interestingly, shifting from two aromatic substituents (**PABA**, $A_{max} = 375$ nm) to one aromatic and one alkynyl group (**PCPA**, **PFPA**, $A_{max} = 391$ nm) and lastly to the two alkynyl groups (**DIPA** $A_{max} = 431$ nm), a bathochromic shift was observed in the absorption spectra, reflecting the effect of the extended conjugation on the aromaticity of these compounds.

The reaction monitoring could be achieved by UV-Vis absorption spectroscopy following the disappearing of the absorption bands of the aromatic substrates upon formation of the EPOs (Figure 3c). Since the formation of the O–O bridge breaks the aromaticity of the central ring of the anthracenes, their characteristic absorption bands in the region between 325 and 450 nm decrease proportionally to the reaction extent. Upon exclusive, quantitative formation of the target EPOs, the final absorption spectra showed only the profile of the PS above 300 nm.

The newly synthesized aromatic substrates **PFPA**, **PCPA** and **DIPA** were quantitatively converted to the corresponding EPOs

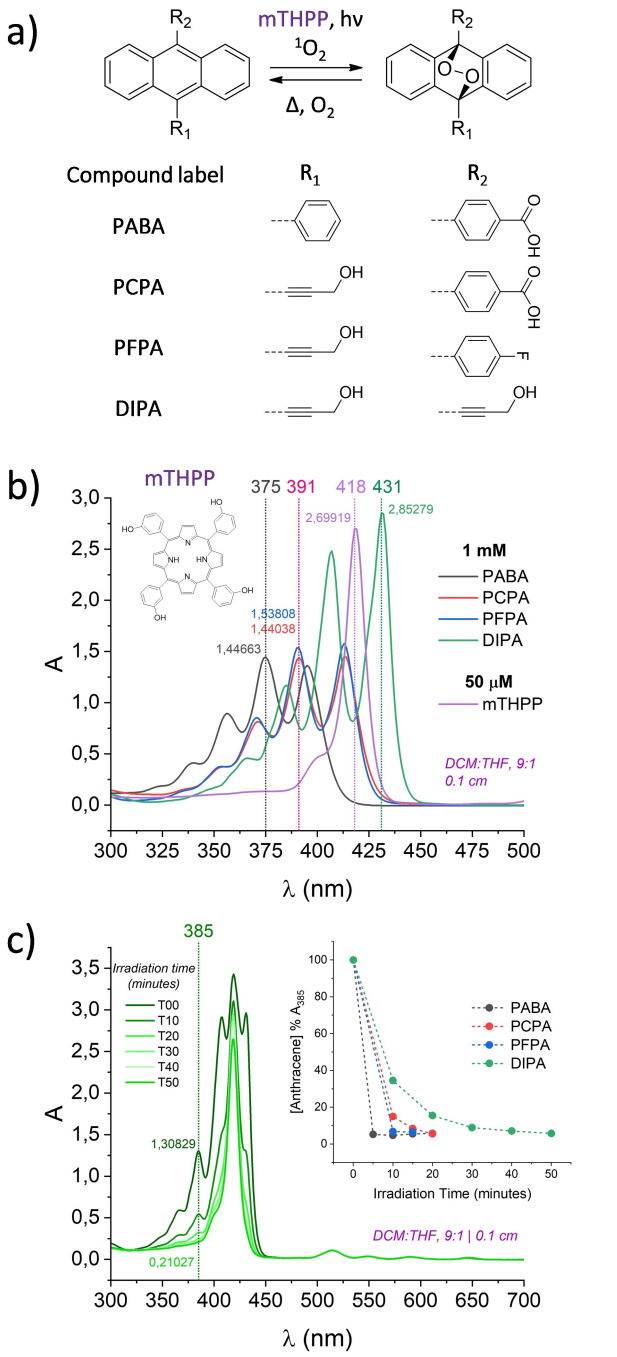

Figure 3. a) General scheme for the reversible binding of photosensitized $^1O_2$ to aromatic substrates; b) UV-Vis absorption spectra (0.1 cm, DCM:THF 9:1) of **PABA**, **PCPA**, **PFPA**, **DIPA** and **mTHPP**; c) UV-Vis absorption spectra (0.1 cm, DCM:THF 9:1) monitoring the photooxygenation of **DIPA** (1 mM) in the presence of 5% mol/mol of mTHPP (1 mL/min *in flow* irradiation, 525 nm LED, $T_{set} = 0\,°C$). Inset: A values (385 nm) of the reaction mixtures during irradiation of the aromatic substrates plotted against the time.

PFPA-O2, **PCPA-O2** and **DIPA-O2** (Figures S9, S10, S11, S12) using the following parameters:

- 5% mol/mol of PS compared to the aromatic substrate
- 100% of intensity of LED lamp emitting at 525 nm
- Flow rate: 0.5, 1 or 2 mL min^{-1}–1
- 5 to 20 minutes of residence time

Research Article
doi.org/10.1002/ejoc.202400861

- T_{set} = 25 °C for all anthracenes except for DIPA, whose corresponding EPO was reverting at room temperature so fast that it required to be irradiated at T_{set} = 0 °C.

Under the set conditions, it was possible to quantitatively convert 1 μmol min^{-1} (corresponding on average to about 0.4 mg min^{-1}) of substrate to EPO.

Cycloreversion Upon Thermolysis: Kinetics of O_2 Release

Purification and isolation of the pure EPOs could not be achieved due to the thermal instability of the molecules. However, considering the low amount of PS (5% mol/mol) and quantitative conversion of the parent substrates, cycloreversion of the EPOs was investigated on the reaction crudes once concentrated to dryness with the use of a Smart Evaporator® working at room temperature under *vacuum*. The obtained solid residues could be stored at −18 °C up to ten days. Despite also **DIPA-O2** was found to be stable in the reaction mixture at −18 °C for over one week (Figure S13), the compound resulted to revert to **DIPA** during solvent removal.

Cycloreversion of EPOs to their corresponding parent compounds was monitored in DMSO using (Figure 4):

- ***UV-Vis:*** to evaluate the kinetics of O_2-release at different temperatures (Figures S9, S10, S11, S12, S14)
- ***1H-NMR:*** to qualitatively confirm the formation of the parent compounds proving the reversibility of the reaction and the lack of side processes (Figures S15, S16, S17).

UV-Vis spectra were collected over a period of 75 minutes at different temperatures set to 25, 37.5, 45 and 50 °C. At 25 °C, only **DIPA-O2** was found to partially start the conversion, while at 45 and 50 °C all the newly synthesized EPOs were found to significantly release O_2. At physiologically relevant temperature, 37.5 °C (Figure 4a), **PABA-O2** did not show any release, while detectable amount of **PFPA** and **PCPA** could be observed. However, **DIPA-O2** outperformed the other candidates showing nearly quantitative conversion to parent **DIPA** in 75 minutes.

In line with these results, the ^{1}H NMR spectra acquired over time of **PCPA-O2**, **PFPA-O2** and **DIPA-O2** stored at 50 °C, showed full recovery of **DIPA** within < 0.5 h and > 75% recovery of **PFPA** and **PCPA** after 35 h. Moreover, the lack of signals related to potential impurities confirmed that the cycloreversion reaction was the only process happening upon thermolysis.

Eventually, UV-Vis data were used to calculate the thermolysis rate constants (k, s^{-1}) as well as the half-life time ($t_{1/2}$) of the EPOs,[20] shown in Table 1 at 37,5 °C. The Activation Energy (AE) for O_2 release was obtained from the Arrhenius plot of each substrate (Figure 4c, Figure S14).

PCPA-O2 and **PFPA-O2** showed overlapping kinetic profiles eventually resulting in similar $t_{1/2}$ ≈ 90 h at 37.5 °C. **DIPA-O2**, instead, showed AE value in line with the thermolysis occurring at room temperature (93 kJ mol^{-1}), confirmed by the calculated $t_{1/2}$ ≈ 40 minutes at 37.5 °C.

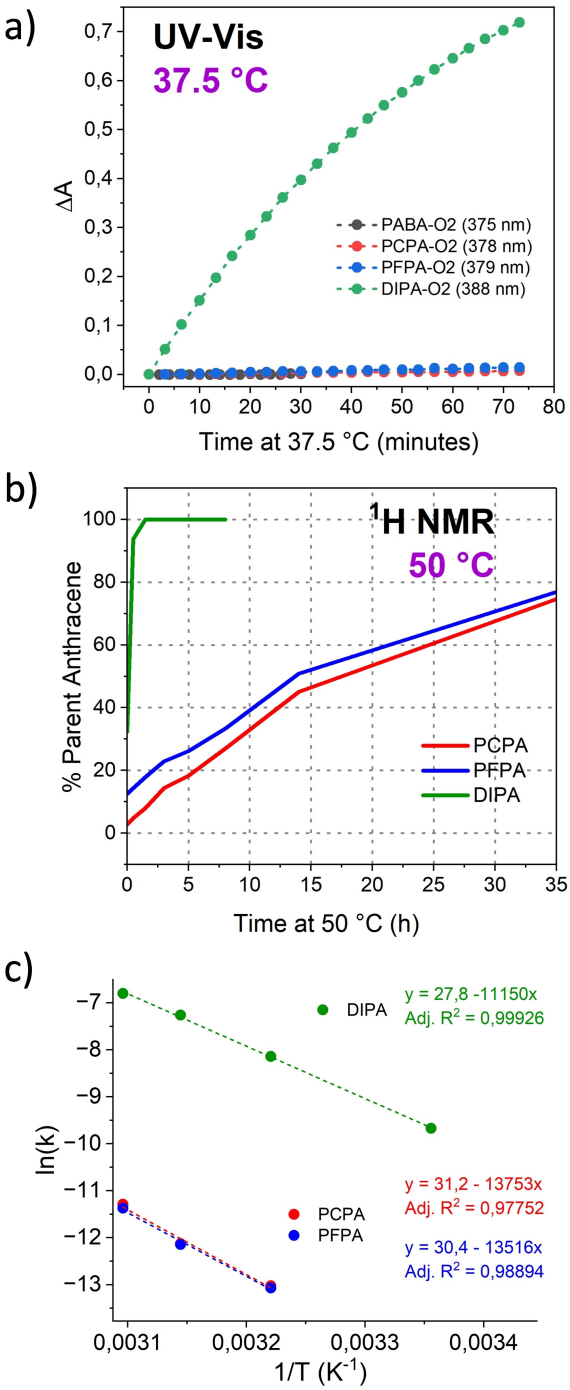

Figure 4. O_2 release monitored by a) UV-Vis at 37.5 °C (DMSO, ΔA = difference between the starting A value and the experimental ones over time); b) ^{1}H NMR (500 MHz, DMSO-d_6) of the compounds stored at 50 °C. c) Arrhenius plots from UV-Vis spectra monitoring the thermolysis of PCPA-O2, PFPA-O2 and DIPA-O2 at 37.5, 45 and 50 °C. For DIPA-O2, also data at 25 °C were included.

Conclusions

This work collected most recent advances on the successful preparation of innovative systems based on aromatic endoperoxides (EPOs) to be used as oxygen-releasing agents (ORAs) in the treatment of hypoxia.

Table 1. Rate constant (k, s^{-1}) and half-life time ($t_{1/2}$) for O_2 release at 37.5 °C and thermolysis activation energy ($kJ\,mol^{-1}$) obtained from UV-Vis data.

Compound	k (s^{-1})	AE ($kJ\,mol^{-1}$)	$t_{1/2}$
DIPA-O2	2.9×10^{-4}	93	40 min
PCPA-O2	2.2×10^{-6}	114	87 h
PFPA-O2	2.1×10^{-6}	113	92 h

Computational DFT data afforded the dissociation energy (E_{diss}) for a series of anthracene-derivatives to be exploited as EPOs. Three anthracene derivatives were selected as suitable candidates based on the calculated values of E_{diss}. **DIPA**, **PCPA**, and **PFPA** were prepared by optimized Sonogashira and Suzuki couplings of alkynyl and/or aromatic substituents in positions 9 and 10 of the anthracene scaffold and the crystallographic analysis of tested structures confirmed the favorable orientation of the appended moieties to accommodate the EPO bridges.

The target EPOs were prepared for the first time using a continuous flow photoreactor in the presence of a sub-stoichiometric amount of photosensitizer (mTHPP).

Thermolysis of the substrates was then proven and monitored by UV-Vis and ^{1}H NMR spectroscopies for all compounds. However, while for **PCPA-O2** and **PFPA-O2** significant O_2 release was achieved only at $T > 45$ °C, the best ORA candidate **DIPA-O2** displayed a $t_{1/2} \approx 40$ minutes already at 37.5 °C.

Further studies on this system are expected to enable their exploitation in physiological media and biocompatible conditions. In fact, solubilization in water with a hydrophilic carrier and *in situ* delivery has been proven to prevent the expected toxicity of anthracene-derivatives and simultaneously to take advantage of their therapeutic effects.[32] Moreover, for the purpose of hypoxia relieving in a combination therapy regime, both $^3O_2$ and $^1O_2$ could serve either as a substrate for PDT or as reactive oxygen species (ROS) itself. Eventually, considering the optical properties of anthracenes, the use of these derivatives could allow not only the treatment of hypoxia to restore the therapeutic performance of commercial drugs, but also the visualization of the readily emitting anthracene derivative for theranostic purposes.

Supporting Information Summary

The authors have cited additional references within the Supporting Information.[33–55]

Crystallographic data for the structures reported in this manuscript have been deposited with the Cambridge Crystallographic Data Centre under the CCDC numbers: 2351990 (**ANBA**), 2351991 (**PABA**), 2351992 (**PABA-O2**), 2351993 (**PNBA**) and 2351994 (**PFPA**). Copies of these data can be obtained free of charge from http://www.ccdc.cam.ac.uk/data_request/cif.

Acknowledgements

The NextGeneration EU Programme is kindly acknowledged for supporting the Ecosystem for Sustainable Transition in Emilia-Romagna (ECOSISTER). The European Union (EU)'s Horizon Europe Research and Innovation Programme is also acknowledged for funding the Marie Sklodowska-Curie grant agreement Bicyclos N° 101130235. Views and opinions expressed are however those of the authors only and do not necessarily reflect those of the EU which cannot be held responsible for them. Open Access Funding was provided by Consiglio Nazionale delle Ricerche (CNR) within the CRUI-CARE Agreement. Open Access publishing facilitated by Consiglio Nazionale delle Ricerche, as part of the Wiley - CRUI-CARE agreement.

Conflict of Interests

The authors declare no conflict of interest.

Data Availability Statement

The data that support the findings of this study are openly available in ChemRxiv at https://doi.org/10.26434/chemrxiv-2024-0nf7j, reference number 0.

Keywords: DFT · Hypoxia · Flow chemistry · Oxygen release · Photochemistry · @MarcoAgnes2, @ilsemanet, @Cnr_Isof, @CNRsocial_

[1] In *Encyclopedic Reference of Genomics and Proteomics in Molecular Medicine*, Springer Berlin Heidelberg, Berlin, Heidelberg, **2006**, 853–853, DOI https://doi.org/10.1007/3-540-29623-9_7440.
[2] A. C. Gonçalves, E. Richiardone, J. Jorge, B. Polónia, C. P. R. Xavier, I. C. Salaroglio, C. Riganti, M. H. Vasconcelos, C. Corbet, A. B. Sarmento-Ribeiro, *Drug Resistance Updates* **2021**, *59*, DOI: 10.1016/j.drup.2021.100797.
[3] F. Marcucci, C. Rumio, *Neoplasia (United States)* **2021**, *23*, 234–245.
[4] B. Schaible, C. T. Taylor, K. Schaffer, *Antimicrob. Agents Chemot < her.* **2012**, *56*, 2114–2118.
[5] C. H. Kowalski, K. A. Morelli, D. Schultz, C. D. Nadell, R. A. Cramer, *Proc. Natl. Acad. Sci. U S A* **2020**, *117*, 22473–22483.
[6] F. Adhami, G. Liao, Y. M. Morozov, A. Schloemer, V. J. Schmithorst, J. N. Lorenz, R. S. Dunn, C. V. Vorhees, M. Wills-Karp, J. L. Degen, R. J. Davis, N. Mizushima, P. Rakic, B. J. Dardzinski, S. K. Holland, F. R. Sharp, C. Y. Kuan, *Am. J. Pathol.* **2006**, *169*, 566–583.
[7] G. Loor, P. T. Schumacker, *Cell Death Differ.* **2008**, *15*, 686–690.
[8] W. Boulefour, E. Rowinski, S. Louati, S. Sotton, A. S. Wozny, P. Moreno-Acosta, B. Mery, C. Rodriguez-Lafrasse, N. Magne, *Med. Sci. Monit.* **2021**, *27*, 1–7.
[9] X. Li, N. Kwon, T. Guo, Z. Liu, J. Yoon, *Angew. Chem. Int. Ed.* **2018**, *57*, 11522–11531.
[10] E. L. Clennan, *Photochem. Photobiol.* **2022**, 1–17.
[11] J.-M. Aubry, C. Pierlot, J. Rigaudy, R. Schmidt, *Acc Chem Res* **2003**, *36*, 668–675.
[12] W. Fudickar, T. Linker, in *PATAI'S Chemistry of Functional Groups*, (Ed.: L. John Wiley & Sons), John Wiley & Sons, Ltd, Chichester, UK, **2014**, 1–66.
[13] W. Fudickar, T. Linker, *Angew. Chem. Int. Ed.* **2018**, *57*, 12971–12975.
[14] W. Fudickar, T. Linker, *Chem. Commun.* **2008**, *15*, 1771–1773.
[15] W. Fudickar, T. Linker, *ChemPhotoChem* **2021**, *5*, 1004–1008.
[16] M. Klaper, T. Linker, *Chem. – Eur. J.* **2015**, *21*, 8569–8577.
[17] W. Fudickar, T. Linker, *ChemPhotoChem* **2018**, *2*, 548–558.
[18] Z. Gao, Y. Han, F. Wang, *Nat. Commun.* **2018**, *9*, 1–9.

[19] D. Zehm, W. Fudickar, T. Linker, *Angew. Chem. Int. Ed.* **2007**, *46*, 7689–7692.
[20] P. De Bonfils, P. Nun, V. Coeffard, *European J Org Chem* **2024**, *202400099*, DOI: 10.1002/ejoc.202400099.
[21] W. Fudickar, T. Linker, *Langmuir* **2010**, *26*, 4421–4428.
[22] M. Agnes, A. Mazza, E. Kalydi, S. Béni, M. Malanga, I. Manet, *Chem.– Eur. J.* **2023**, *29*, DOI: 10.1002/chem.202300511.
[23] S. Kolemen, T. Ozdemir, D. Lee, G. M. Kim, T. Karatas, J. Yoon, E. U. Akkaya, *Angew. Chem. Int. Ed.* **2016**, *55*, 3606–3610.
[24] W. Fudickar, T. Linker, *Chem. – Eur. J.* **2011**, *17*, 13661–13664.
[25] W. Fudickar, T. Linker, *J. Am. Chem. Soc.* **2012**, *134*, 15071–15082.
[26] D. Lovison, D. Alessi, L. Allegri, F. Baldan, M. Ballico, G. Damante, M. Galasso, D. Guardavaccaro, S. Ruggieri, A. Melchior, D. Veclani, C. Nardon, W. Baratta, *Chem. – Eur. J.* **2022**, *28*, e202200200.
[27] H. L. te Vrugt, R. Wittkowski, *Adv. Phys.* **2020**, *69*, 121–247.
[28] P. Verma, D. G. Truhlar, *Trends Chem.* **2020**, *2*, 302–318.
[29] C. F. R. A. C. Lima, L. R. Gomes, L. M. N. B. F. Santos, J. N. Low, *Acta Crystallogr. Sect E Struct. Rep. Online* **2009**, *65*, o3037–o3037.
[30] M. B. Plutschack, B. Pieber, K. Gilmore, P. H. Seeberger, *Chem. Rev.* **2017**, *117*, 11796–11893.
[31] L. Capaldo, Z. Wen, T. Noël, *Chem Sci.* **2023**, *14*, 4230–4247.
[32] G. R. Choppin, S. A. Khan, G. C. Levy, *Spectrosc. Lett.* **1980**, *13*, 205–210.
[33] M. J. Frisch, G. W. Trucks, H. B. Schlegel, G. E. Scuseria, M. A. Robb, J. R. Cheeseman, G. Scalmani, V. Barone, G. A. Petersson, H. Nakatsuji, X. Li, M. Caricato, A. V. Marenich, J. Bloino, B. G. Janesko, R. Gomperts, B. Mennucci, H. P. Hratchian, J. V. Ortiz, A. F. Izmaylov, J. L. Sonnenberg, D. Williams-Yung, F. Ding, F. Lipparini, F. Egidi, J. Goings, B. Peng, A. Petrone, T. Henderson, D. Ranasinghe, V. G. Zakrzewski, J. Gao, N. Rega, G. Zheng, W. Liang, M. Hada, M. Ehara, K. Toyota, R. Fukuda, J. Hasegawa, M. Ishida, T. Nakajima, Y. Honda, O. Kitao, H. Nakai, T. Vreven, K. Throssell, J. A. Montgomery Jr., J. E. Peralta, F. Ogliaro, M. Bearpark, J. J. Heyd, E. Brothers, K. N. Kudin, V. N. Staroverov, T. A. Keith, R. Kobayashi, J. Normand, K. Raghavachari, A. Rendell, J. C. Burant, S. S. Iyengar, J. Tomasi, M. Cossi, J. M. Millam, M. Klene, C. Adamo, R. Cammi, J. W. Ochterski, R. L. Martin, K. Morokuma, O. Farkas, J. B. Foresman, D. J. Fox, *Gaussian 16 Revision A 03* **2016**.
[34] C. Lee, W. Yang, R. G. Parr, *Phys. Rev. B* **1988**, *37*, 785–789.
[35] S. H. Vosko, L. Wilk, M. Nusair, *Can. J. Phys.* **1980**, *58*, 1200–1211.
[36] P. J. Stephens, F. J. Devlin, C. F. Chabalowski, M. J. Frisch, *J. Phys. Chem.* **1994**, *98*, 11623–11627.
[37] A. D. Becke, *J. Chem. Phys.* **1993**, *98*, 5648–5652.
[38] F. Weigend, *Phys. Chem. Chem. Phys.* **2006**, *8*, 1057–1065.
[39] F. Weigend, R. Ahlrichs, *Phys. Chem. Chem. Phys.* **2005**, *7*, 3297–3305.
[40] W. Fudickar, T. Linker, *J. Phys. Org. Chem.* **2019**, *32*, e3951.
[41] Y.-Q. He, W. Fudickar, J.-H. Tang, H. Wang, X. Li, J. Han, Z. Wang, M. Liu, Y.-W. Zhong, T. Linker, P. J. Stang, *J. Am. Chem. Soc.* **2020**, *142*, 2601–2608.
[42] A. Putta, A. G. Sykes, H. Sun, *J. Fluor Chem.* **2020**, *235*, 109548.
[43] M.-P. Minadakis, K. F. Mavreas, D. D. Neofytos, M. Paschou, A. Kogkaki, V. Athanasiou, M. Mamais, D. Veclani, H. Iatrou, A. Venturini, E. D. Chrysina, P. Papazafiri, T. Gimisis, *Org. Biomol. Chem.* **2022**, *20*, 2407–2423.
[44] B. Ventura, D. Veclani, A. Venturini, N. Armaroli, M. Baroncini, P. Ceroni, M. Marchini, *Chem. – Eur. J.* **2023**, *29*, e202301853.
[45] B. Mennucci, J. Tomasi, R. Cammi, J. R. Cheeseman, M. J. Frisch, F. J. Devlin, S. Gabriel, P. J. Stephens, *J. Phys. Chem. A* **2002**, *106*, 6102–6113.
[46] S. F. Boys, F. Bernardi, *Mol. Phys.* **1970**, *19*, 553–566.
[47] E. R. Johnson, S. Keinan, P. Mori-Sánchez, J. Contreras-García, A. J. Cohen, W. Yang, *J. Am. Chem. Soc.* **2010**, *132*, 6498–6506.
[48] J. Contreras-García, E. R. Johnson, S. Keinan, R. Chaudret, J.-P. Piquemal, D. N. Beratan, W. Yang, *J. Chem. Theory Comput.* **2011**, *7*, 625–632.
[49] M. (WI) APEX3 Software Package V2019, Bruker AXS Inc., **2019**.
[50] M. (WI) Bruker SAINT, v8.40 A: Part of the APEX3 Software Package V2019, Bruker AXS Inc., **2019**.
[51] M. (WI) Bruker SADABS V2016/2: Part of the APEX3 Software Package V2019, Bruker AXS Inc., **2019**.
[52] G. M. Sheldrick, *Acta Crystallogr. A Found Adv.* **2015**, *71*, 3–8.
[53] G. M. Sheldrick, *Acta Crystallogr. Section C* **2015**, *71*, 3–8.
[54] A. L. Spek, *Acta Crystallogr Section C* **2015**, *71*, 9–18.
[55] C. F. Macrae, I. Sovago, S. J. Cottrell, P. T. A. Galek, P. McCabe, E. Pidcock, M. Platings, G. P. Shields, J. S. Stevens, M. Towler, P. A. Wood, *J. Appl. Crystallogr.* **2020**, *53*, 226–235.

Manuscript received: July 30, 2024
Revised manuscript received: August 19, 2024
Accepted manuscript online: August 19, 2024
Version of record online: September 18, 2024